Preprints.org

Article

Not peer-reviewed version

Effect of Acoustic Pressure on Temozolomide-Loaded Oleic Acid-Based Liposomes and Its Safety to Brain Tissue

Vasilisa D. Dalinina , Vera S. Shashkovskaya * , Iman M Khaskhanova , Daria Yu Travnikova , Nelly S Chmelyuk , Dmitry A Korzhenevskiy , Vsevolod V Belousov , Tatiana O Abakumova *

Posted Date: 13 May 2025

doi: 10.20944/preprints202505.0973.v1

Keywords: liposomes; oleic acid; temozolomide; focused ultrasound; blood–brain barrier; glioma; drug delivery; controlled release

Preprints.org is a free multidisciplinary platform providing preprint service that is dedicated to making early versions of research outputs permanently available and citable. Preprints posted at Preprints.org appear in Web of Science, Crossref, Google Scholar, Scilit, Europe PMC.

Copyright: This open access article is published under a Creative Commons CC BY 4.0 license, which permit the free download, distribution, and reuse, provided that the author and preprint are cited in any reuse.

Preprints.org (www.preprints.org) | NOT PEER-REVIEWED | Posted: 13 May 2025 doi:10.20944/preprints202505.0973.v1

Disclaimer/Publisher's Note: The statements, opinions, and data contained in all publications are solely those of the individual author(s) and contributor(s) and not of MDPI and/or the editor(s). MDPI and/or the editor(s) disclaim responsibility for any injury to people or property resulting from any ideas, methods, instructions, or products referred to in the content.

Article

Effect of Acoustic Pressure on Temozolomide-Loaded Oleic Acid-Based Liposomes and Its Safety to Brain Tissue

Vasilisa D. Dalinina [1,†], Vera S. Shashkovskaya [1,*,†], Iman M. Khaskhanova [1], Daria Yu. Travnikova [1], Nelly S. Chmelyuk [1], Dmitry A. Korzhenevskiy [2], Vsevolod V. Belousov [1,2] and Tatiana O. Abakumova [1,*]

[1] Pirogov Russian National Medical University, 117997 Moscow, Russia
[2] Federal Center of Brain Research and Neurotechnologies, Federal Medical Biological Agency, 119435 Moscow, Russia
* Correspondence: verashashkovskaya@gmail.com (V.S.S.); sandalovato@gmail.com (T.O.A.)
† These authors contributed equally to this work.

Abstract: Glioblastoma (GBM) is a highly aggressive primary brain tumor with limited therapeutic options, particularly due to the limited blood-brain barrier (BBB) permeability. Nanoparticle-based drug delivery systems, such as liposomes, can prolong drug circulation time and enhance accumulation within brain tumors, thereby improving therapeutic outcomes. Controlled drug release further contributes to high local drug concentrations while minimizing systemic toxicity. Oleic acid (OA), a monounsaturated fatty acid, is commonly used to enhance drug loading, and increase lipid membrane fluidity. In this study, we developed liposomal formulations with varying lipid compositions to optimize temozolomide (TMZ) loading and analyze its response to focused ultrasound (FUS). All formulations exhibited comparable hydrodynamic diameters; however, OA-containing liposomes demonstrated significantly higher TMZ encapsulation efficiency and enhanced cytotoxicity in U87 glioma cells. Moreover, it was shown that OA-liposomes were disrupted at lower acoustic pressures (5 MPa), while conventional liposomes required higher thresholds (>8 MPa). Safety analysis of FUS parameters indicated that pressures exceeding 11 MPa induced brain edema, necrotic lesions, and elevated cytokine levels within 72 hours post-treatment. These results suggest that OA-based liposomes possess favorable characteristics with increased sonosensitivity for site-specific delivery of TMZ, offering a promising strategy for glioma treatment.

Keywords: liposomes; oleic acid; temozolomide; focused ultrasound; blood–brain barrier; glioma; drug delivery; controlled release

1. Introduction

Low-grade gliomas are the most common subtype of CNS tumors with high rate of relapse and mortality (5-year survival rate of less than 30%) [1,2]. Current chemotherapy approaches are insufficient mostly due to the limited sensitivity, low stability, rapid clearance, poor solubility, high systemic toxicity of drugs, as well as limited permeability of the blood-brain barrier (BBB) in the tumor lead to insufficient drug concentrations. Several approaches have been developed to increase the drug concentration in the tumor in order to reduce systemic toxicity to the body, one of them is nanoparticles-based delivery systems with triggered-systems drug delivery. Controlled drug release can be carried out under the influence of both internal and external stimuli such as pH, the presence of active forms of oxygen, enzymes, for example phospholipases, proteinase or other specific enzymes, temperature, magnetic field, radioactive radiation, light radiation and ultrasound radiation [3–5]. The main limiting factor of internal stimuli is the heterogeneity of tumor cells and tissues. The disadvantage of radioactive exposure can be called low safety with a fairly good depth of radiation penetration, while light radiation is the safest, but its use is limited due to the small depth of

© 2025 by the author(s). Distributed under a Creative Commons CC BY license.

Preprints.org (www.preprints.org) | NOT PEER-REVIEWED | Posted: 13 May 2025 doi:10.20944/preprints202505.0973.v1

penetration. Magnetic field and ultrasound radiation have the most safety and effectiveness. All of these approaches have shown its efficacy in the treatment of various tumors (prostate cancer, breast cancer, hepatocellular carcinoma and other) with more than 300 ongoing clinical studies with nanoparticles for therapy against tumors and other diseases [6].

The use of nanoparticles in glioblastoma treatment is a complex task that is primarily limited by the low BBB permeability. Despite the fact that brain tumors are associated with compromised BBB integrity (abnormal vascular growth, destruction of tight contacts between cells), the permeability through vascular vessels is uneven. High heterogeneity is associated with the features of tumor growth, intracellular pressure, hypoxia area and other factors [7]. Moreover, glioblastoma is characterized by diffuse growth of cancer cells into healthy tissue and the BBB in the peritumoral zone remains mostly intact. These areas cannot be completely surgically removed and should be reduced by the following radio- and chemotherapy.

Temozolomide (TMZ) is the standard of chemotherapy for the treatment of glioblastomas. Its advantage is the ability to penetrate the BBB (20-40% of the concentration in blood plasma), while its main disadvantage is its safety profile [8,9]. TMZ is stable at acidic pH values and is hydrolyzed under physiological conditions (pH 7.4) to the active component 3-methyl-(triazene-1)-imidazole-4 carboximide (MTIC), which further methylates DNA and leads to apoptosis of the tumor cell. To prevent fast degradation of TMZ and maintain its therapeutic concentration in tumor, nanoparticles could be utilized [10].

Liposomes are an effective drug delivery system both for hydrophilic and hydrophobic drugs that have been successfully translated to the clinic [11]. Doxorubicin-loaded liposomes (Caelyx) have demonstrated their efficacy in the Phase II trial in combination with TMZ [12]. Various studies have demonstrated that TMZ can be sufficiently encapsulated into liposomes with average efficiency of 35-45% and proved its efficacy in comparison with free TMZ [13]. Tejashree Waghule et al (2023) showed the TMZ-loaded lipid-based nanocarriers significantly prolonged blood circulation time of TMZ [14]. Nerea Iturrioz-Rodríguez1 et al. (2023) discussed the different strategies to overcome limitation of TMZ-loaded nanoparticles including its loading efficiency [15]. Previously, it was shown that various parameters could affect drug loading in liposomes, including specific phospholipid features (acyl chain length, side chains, charge and the phase transition temperature [16]. Oleic acid (OA) as well as other unsaturated fatty acid was extensively studied as a surfactant or co-solvent for hydrophobic drugs such as TMZ as well as a component of liposomes [17,18]. Previously, it was shown that liposomes with OA demonstrated better encapsulation efficiency (EE) (more than 60%) [19]. Also, it was shown that oleic acid could enhance therapeutic effect by suppressing glutathione peroxidase 4 (GPX4) [20]. Important part, that incorporation of unsaturated fatty acid can impact on fluidity and stiffness of lipid membranes and destabilize them that could be utilized in controlled drug release [21].

Focused ultrasound (FUS) is a safe and easily adaptable external stimulus that could improve the effectiveness of nanomedicine in glioblastoma therapy [22]. It can be used in two modes: high-intensity focused ultrasound (HIFU) and low-intensity focused ultrasound (LIFU). The use of thermosensitive components, such as polymers or lipids, can trigger the release of a substance, while non-thermal methods mostly rely on the inertial cavitation effect, which is a mechanical effect. This approach can reduce the systemic toxicity of a drug by controlling its release only in the pathological area, thus increasing the local delivery of the drug. LIFU is another approach to increase the accumulation of drugs, including ultrasound-inert nanoparticles in the brain. Injection of gas-filled microbubbles followed with transcranial sonication has proved its efficacy to deliver anticancer drugs (TMZ, doxorubicin, carboplatin, etc.) to brain tumors. This approach has also shown its effectiveness for the delivery of nanoparticles. Thus, when exposed to ultrasound, a 6-40-fold increase in the accumulation of cisplatin particles (60 nm particles) was shown, 1.4-6.9-fold increase in accumulation for particles with paclitaxel (170 nm particles) [23,24].

The development of a combined approach that makes it possible to improve modern methods of glioblastoma therapy using nanotechnology is the most rational step to increase the life expectancy

© 2025 by the author(s). Distributed under a Creative Commons CC BY license.

Preprints.org (www.preprints.org) | NOT PEER-REVIEWED | Posted: 13 May 2025 doi:10.20944/preprints202505.0973.v1

of patients. Here we investigated TMZ-loaded liposomes with increased entrapment efficiency, stimuli-sensitive release and delivery using different application modes of focused ultrasound.

2. Results and Discussion

2.1. Synthesis and Characterization of Oleic-Based Liposomes

Liposomes are promising drug carriers due to their mechanical strength, flexibility, low toxicity, and high biocompatibility [25]. Previous studies have demonstrated that liposomal TMZ can significantly improve the accumulation of TMZ in glioma tissue [26]. In this study we synthesized liposomes with various lipid compositions to develop either neutral or cationic nanoformulations. Specifically, we incorporated DDAB to investigate the effect of cationic lipids on delivery of TMZ to glioma cells. Additionally, OA was included in the formulations as the previous research showed its potential as co-solvent of hydrophobic drugs, which could enhance entrapment efficiency [27].

All liposome formulations exhibited a similar size distribution with particle size less than 200 nm. However, the incorporation of OA or DDAB resulted in a slight increase of the hydrodynamic diameter of liposomes. Notably, a ten-fold increase in the molar ratio of OA to cholesterol led to increase in nanoparticle size compared to the liposomes without OA (from ≈160 to ≈190 nm). Zeta-potential measurements revealed that OA-containing liposomes had a more negative charge compared to the conventional liposomes, while the incorporation of DDAB led to the positive zeta potential of the nanoparticles (Figure 1A). TEM images confirmed the liposome retained a spherical morphology and had size less than 200 nm (Figure S1). Both OA-based and conventional liposomal formulations were stable for up to 48 hours (Figure 1C), though OA-based liposomes demonstrated a notable increase in PDI after 72 hours.

We next evaluated the encapsulation efficiency (EE) and loading capacity (LC) of the liposomal formulations. To quantify TMZ in different liposome formulations, we compared two methods: mass spectrometry (HPLC-MS) and spectrophotometry. The spectrophotometric method involved measuring TMZ in either the waste solution (collected from purification step as non-entrapped drug) or the extracted phase (disrupted Lip-TMZ) —methods commonly used in the literature. Interestingly, spectrophotometric measurements revealed that the calculated EE for TMZ exceeded 60% for all formulations (Table S3), which aligns with other studies. However, HPLC-MS, which provided a more precise measurement of both TMZ and its metabolite (AIC), yielded more reliable results. We found that the EE of TMZ in OA-based liposomes, with a ten-fold increase in the OA-to-cholesterol molar ratio, was higher (43.1%) compared to liposomes with equal OA-to-cholesterol ratios (19.6%). For instance, the phospholipid–cholesterol liposomes developed by Jinhua Gao et al. achieved an EE and LC of 35.45 ± 1.48% and 2.81 ± 0.20% respectively [28]. In this work, the maximum of EE and LC were achieved for OA-based liposomes and were equal 43.1 ± 2.5% and 0.90 ± 0.03% respectively.

© 2025 by the author(s). Distributed under a Creative Commons CC BY license.

Preprints.org (www.preprints.org) | NOT PEER-REVIEWED | Posted: 13 May 2025 doi:10.20944/preprints202505.0973.v1

A

Particle type	PDI	Size (nm)	Zeta potential (mV)	EE (%)
Lip	0.26 ± 0.06	162 ± 18	-17 ± 1	21.44
Lip-DDAB	0.27 ± 0.01	172 ± 6	58 ± 1	14.44
Lip-OA 1:1	0.21 ± 0.03	191 ± 33	-35 ± 2	19.6
Lip-OA 1:10	0.23± 0.11	177 ± 18	-42 ± 5	43.1

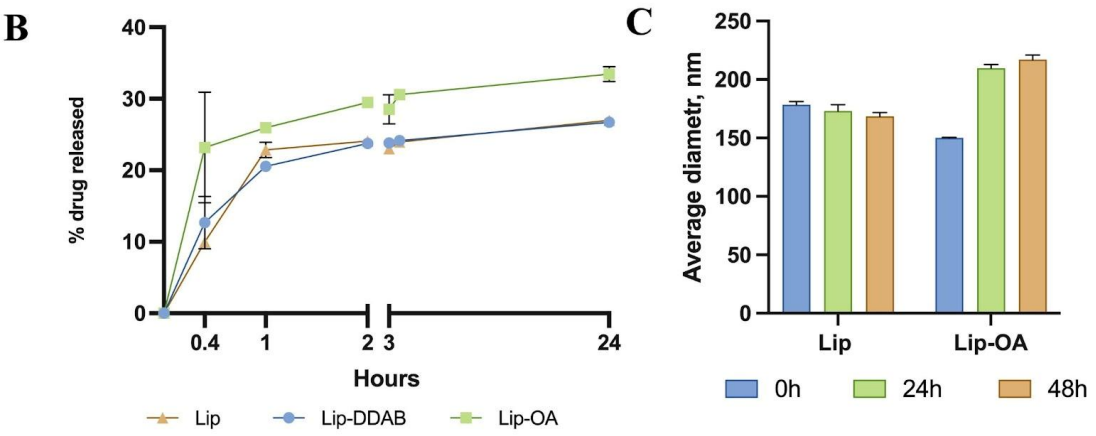

Figure 1. (A) Hydrodynamic size, PDI, zeta-potential and EE of neutral (Lip), cationic (Lip-DDAB) and OA-based liposomes with different molar ratio to cholesterol (Lip-OA 1:1 and Lip-OA 1:10), mean ± SD, n = 3; (B) Drug release of neutral (Lip), cationic (Lip-DDAB) and OA-based liposomes in 24 hours; (C) stability of conventional and OA-based liposomes samples measured by DLS in 24 and 48 hours, mean ± SD, n = 3, n - number of measurements.

To further improve the drug loading efficiency of OA-based liposomes, we employed a double-loading approach. Initially, TMZ was incorporated into the lipid mixture as a premix with OA, serving as a co-solvent. The lipid films were then dissolved in the TMZ solution and subjected to sonication for 5 minutes to encapsulate the drug within the inner aqueous compartment of the liposome. This double-loading method resulted in a two-fold increase in EE (39.8%) in OA-based liposomes with an equal molar ratio of OA and cholesterol, compared to the single-loaded liposomes (19,6%). Interestingly, double-loading did not significantly affect the EE of TMZ in OA-based liposomes with a ten-fold increase in the molar ratio of OA to cholesterol, which remained similar to the single-loaded formulation (43,1% vs. 46,7%) as was detected by HPLC-MS. Notably, double-loaded (DL) liposomes exhibited larger sizes, higher EE, and LC values, along with slower TMZ release compared to single-loaded (SL) liposomes. Furthermore, DL liposomes with an equal OA-to-cholesterol molar ratio demonstrated a greater cytotoxic effect on U87 glioma cell cultures compared to their single-loaded counterparts (Figure 2C). However, no significant difference in cytotoxicity was observed between the DL and SL liposomes containing a 1:10 OA-to-cholesterol ratio.

© 2025 by the author(s). Distributed under a Creative Commons CC BY license.

Preprints.org (www.preprints.org) | NOT PEER-REVIEWED | Posted: 13 May 2025 doi:10.20944/preprints202505.0973.v1

A

Particle type	PDI	Size (nm)	Zeta potential (mV)	EE (%)
Lip-OA 1:1 Dl	0.19 ± 0.01	151 ± 3	-36 ± 1	39.8
Lip-OA 1:10 Dl	0.23 ± 0.11	185 ± 38	-41 ± 1	46.7

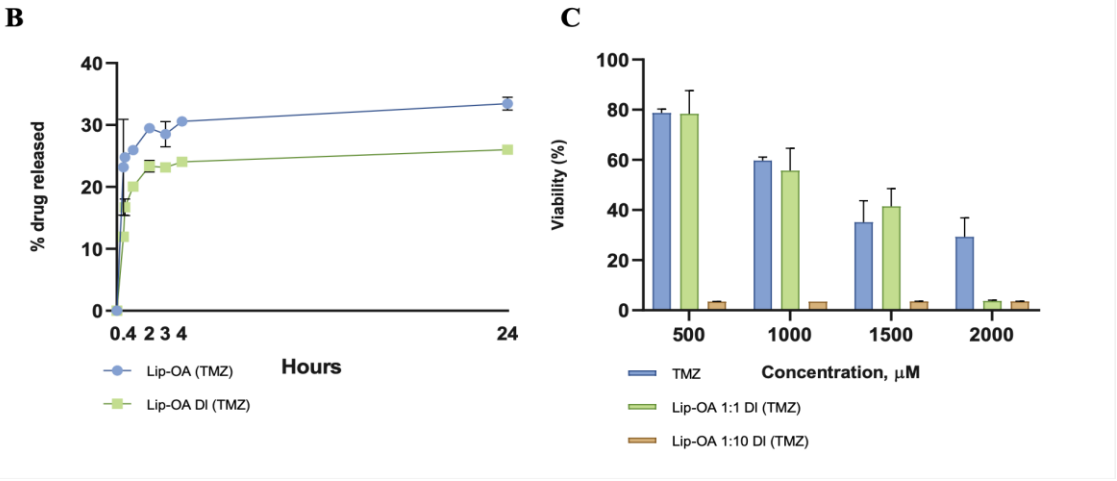

Figure 2. (A) Hydrodynamic size, PDI, zeta-potential and EE of Dl OA-based liposomes with equal (Lip-OA 1:1 Dl) and tenfold increase of molar ratio to cholesterol (Lip-OA 1:10 Dl), mean ± SD, n = 3; (B) The drug release from Sl and Dl OA-based liposomes in 24 hours; (C) The cytotoxicity of TMZ and Dl OA-based liposomes with different ratio of OA to cholesterol on U87 cells, mean ± SD, n = 6.

2.2. In Vitro Cytotoxicity of TMZ-Loaded Liposomes

As the next step in our study, we decided to investigate the cytotoxicity of obtained nanoformulations. Human U87 glioma cells were treated with the various liposome formulations—neutral (Lip), cationic (Lip-DDAB), and OA-based liposomes with varying OA-to-cholesterol molar ratios—along with free TMZ for a duration of 4 days. The results revealed that the cationic liposomes and the OA-based liposomes with a ten-fold increase in the molar ratio of OA to cholesterol exhibited significantly higher cytotoxicity at all drug concentrations when compared to the control groups. This enhanced toxicity is likely attributable to increased cellular uptake of these formulations. Interestingly, the conventional liposomes and the OA-based liposomes with an equal molar ratio of OA to cholesterol did not show any significant increase in cytotoxicity when compared to free TMZ (Figure 3). Moreover, both conventional and cationic liposomes, without the encapsulated drug, did not induce toxicity in U87 cells.

© 2025 by the author(s). Distributed under a Creative Commons CC BY license.

Preprints.org (www.preprints.org) | NOT PEER-REVIEWED | Posted: 13 May 2025 doi:10.20944/preprints202505.0973.v1

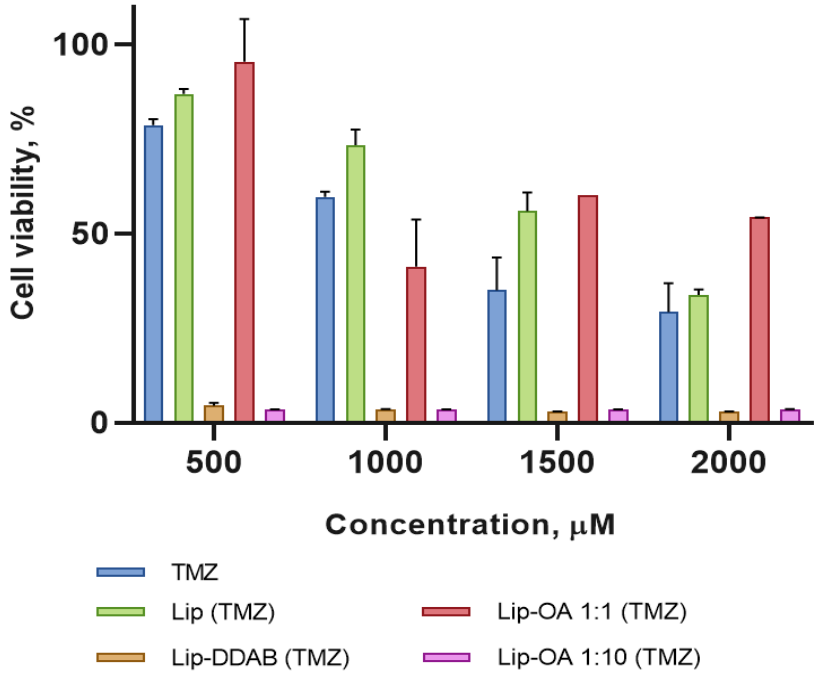

Figure 3. Cytotoxicity of TMZ, conventional liposomes with incorporated TMZ (Lip (TMZ)), OA-based liposomes with incorporated TMZ and equal (Lip-OA 1:1 (TMZ)) and tenfold increase of molar ratio of OA to cholesterol (Lip-OA 1:10 (TMZ) and cationic liposomes with incorporated TMZ (Lip-DDAB (TMZ)) on U87 glioma cells in 96 hours.

Thus, we explored several strategies to improve the loading efficiency of liposomal TMZ, including the incorporation of OA and a two-step loading method. OA has previously been shown to enhance the loading of poorly soluble drugs such as ciprofloxacin, clofazimine and diclofenac [29–31]. OA may also enhance the tumor accumulation of TMZ, as supported by studies demonstrating improved drug delivery and survival when TMZ is conjugated with unsaturated fatty acids [32–34]

2.3. Effect of Acoustic Pressure on Liposome Stability by Focused Ultrasound

FUS can exert multiple effects depending on the acoustic parameters: cavitation, mechanical (non-thermal) effects, and thermal effects. For drug delivery applications, cavitation and mechanical effects are most relevant, as they enable controlled release without damaging surrounding tissues. Several studies have demonstrated that modifying lipid composition of liposomes can enhance their ultrasound responsiveness. OA is known to increase membrane fluidity by disrupting ordered lipid structures such as raft domains. Onuki et al. demonstrated that incorporating 30% OA significantly enhanced the fluidity of DPPC membranes [35]. In our study, the inclusion of OA in liposomal formulations resulted in higher loading capacity (LC) compared to conventional neutral or cationic TMZ-loaded liposomes and we supposed that the incorporation of oleic acid could improve its sonosensitivity.

First, we aimed to assess the impact of FUS on obtained liposome stability, we selected optimal parameters by monitoring the temperature changes in water samples. The temperature increase was kept within a range of 1-3°C to ensure that the liposomes sensitive drug release properties were not compromised (Table S1). Based on these findings, we selected the following parameters for further experimentation: PRF of 5 Hz, pressures of 4.45 MPa and 8.03 MPa, an exposure time of 60 seconds, and a duty cycle of 5%.

Next, we investigated the effect of these optimized FUS parameters on the structural integrity of liposomes. We compared the behavior of conventional liposomes with OA-based liposomes, and LNPs were included as a control [36]. The temperature rise during the FUS treatment was monitored

© 2025 by the author(s). Distributed under a Creative Commons CC BY license.

Preprints.org (www.preprints.org) | NOT PEER-REVIEWED | Posted: 13 May 2025 doi:10.20944/preprints202505.0973.v1

(Table S1). Following the 60-second FUS treatment, we assessed liposomes destruction using dynamic light scattering (DLS). We observed that at the minimum FUS parameters (1 Hz and 5.83 MPa), no particle destruction occurred in either the LNP or conventional liposomes, while OA-coated liposomes showed signs of degradation: the value of maximum of size distribution was increased and/or size distribution was bimodal. At a 5 Hz PRF and 8.03 MPa, both conventional liposomes and OA-based liposomes were significantly disrupted compared to the control group, while LNPs remained intact. At the highest FUS parameters (5 Hz and 11 MPa), all liposomal formulations, including conventional liposomes and OA-coated liposomes, were destroyed, whereas the control LNPs remained stable (Figure 4). These results highlight that the effectiveness of FUS in disrupting liposomes and promoting drug release is influenced by both the PRF and pressure, with OA-based liposomes exhibiting enhanced sensitivity to FUS compared to conventional formulations.

Thus, it can be stated that the introduction of OA into the composition of lipids for liposomes allows to increase their mobility and ability to be destroyed. Similar data were obtained earlier when introducing unsaturated phospholipids into the composition of liposomes. For example, the incorporation of phospholipids with unsaturated acyl chains can destabilize the lipid bilayer, increasing its sensitivity to FUS [37]. Ultrasound-triggered release of cisplatin from modified liposomes has been shown in murine C26 colon adenocarcinoma models. Additionally, the inclusion of PEGylated lipids may further enhance ultrasound sensitivity, possibly by absorbing ultrasonic energy and concentrating it at the liposome surface [38]. Building on this work, our study suggests that OA-containing liposomes may exhibit enhanced ultrasound sensitivity, leading to improved TMZ delivery to glioma tissue. We observed that OA incorporation not only increased TMZ encapsulation but also improved ultrasound-triggered release compared to conventional liposomes.

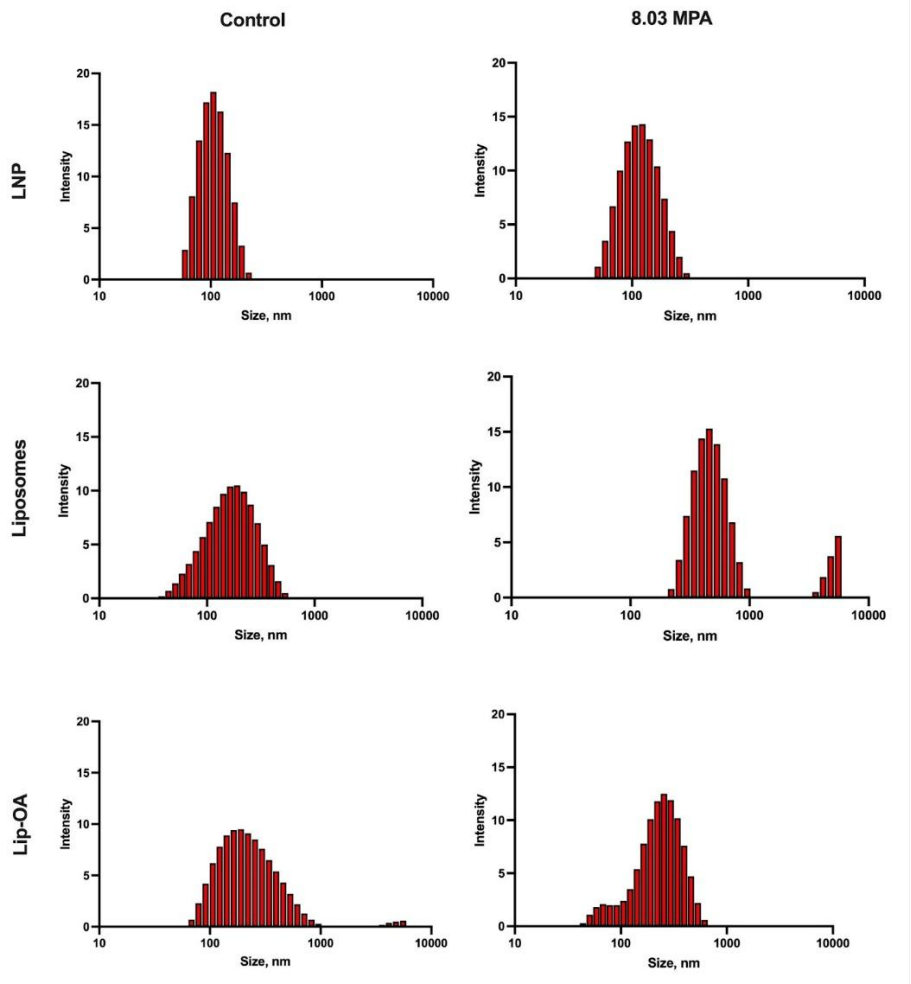

Figure 4. The size distribution of acoustic inert liposomes, lip-OA and LNP before and after sonication with FUS.

© 2025 by the author(s). Distributed under a Creative Commons CC BY license.

Preprints.org (www.preprints.org) | NOT PEER-REVIEWED | Posted: 13 May 2025 doi:10.20944/preprints202505.0973.v1

2.4. Safety of Focused Ultrasound on Brain Tissue and Biodistribution of Synthesized Liposomes

In previous studies, we identified optimal FUS parameters that did not induce significant heating of the surrounding tissue (Table S1). These parameters were effective in the destruction of oleic-based liposomes in vitro (Figure 4), but their safety profile in vivo remained to be fully assessed. To explore the safety parameters associated with ultrasonic particle destruction, we employed four distinct treatment regimens (Table 3) to investigate the impact of these parameters on brain tissue.

MRI scans were performed at two time points: 3 hours and 72 hours after sonication. T2-weighted images of the brains of mice (n=6 per group) were used to assess the presence of any abnormal tissue alterations. At the 3-hour groups 3 (10 MPa) and 4 (11 MPa) showed hyperintense foci on the MRI scans, suggesting the development of edema and inflammation (Figure S3). These findings indicated that tissue damage had occurred shortly after FUS exposure.

For a more detailed pathological assessment, histological analysis was conducted on brain tissue sections stained with hematoxylin-eosin at two time points: 6 hours (acute phase) and 3 days (delayed phase) after sonication. At the 6 hours higher FUS pressures (10 and 11 MPa) were associated with significant tissue damage, including necrosis, pericellular edema, and localized hemorrhages (Figure 5A). High magnification images revealed necrosis surrounding the central lesion area, indicating a more extensive tissue injury than what was evident on the MRI scans at this stage. These findings underscore the need for more precise imaging techniques to detect widespread damage at early time points. We also assessed the cytokine expression levels in brain homogenates to measure the inflammatory response to FUS exposure. Specifically, real-time PCR was used to quantify IL-1α, TNF-α, IL-17, and CCL2 cytokine levels. The results revealed a significant increase in the expression of TNF-α and IL-1α at 72 hours post-FUS treatment, particularly at higher power levels (10 and 11 MPa) (Figure 5C). Lower power levels (6 and 8 MPa) induced a less pronounced effect. Additionally, IL-17 expression peaked at 72 hours, with the highest levels observed at 10 and 11 MPa, further suggesting its involvement in the inflammatory response. Similarly, CCL2 mRNA levels reached their maximum at 72 hours, particularly at the highest ultrasound pressures (11 MPa). These cytokine expression patterns corresponded with the MRI and histological findings, confirming the presence of an inflammatory response and immune system activation, particularly in the higher pressure groups (3 and 4). The substantial increase in inflammatory markers indicates the importance of carefully controlling the FUS parameters to avoid excessive tissue damage and immune system activation. This study demonstrated the critical importance of optimizing multiple FUS parameters, including ultrasound power, pressure, and exposure time, to balance therapeutic efficacy with tissue safety. These results are crucial for translating FUS-based therapies into clinical practice, ensuring that focused ultrasound can be applied effectively without inducing undue harm to surrounding tissues.

© 2025 by the author(s). Distributed under a Creative Commons CC BY license.

Preprints.org (www.preprints.org) | NOT PEER-REVIEWED | Posted: 13 May 2025 doi:10.20944/preprints202505.0973.v1

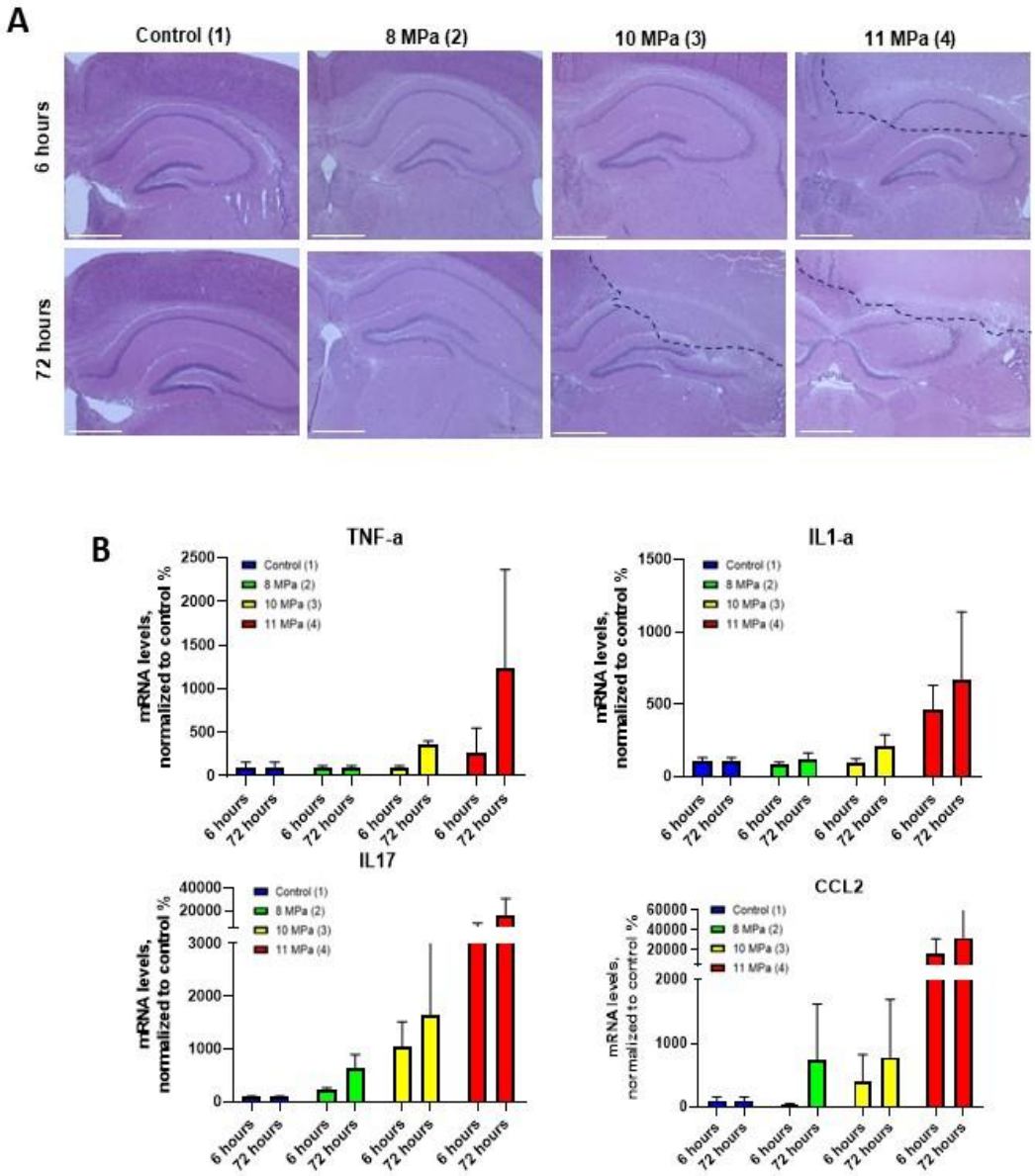

Figure 5. (A) Histological images of mouse brain sections after exposure to FUS with various parameters using hematoxylin-eosin staining. (B) Analysis of the mRNA expression of cytokine markers of inflammation: tumor necrosis factor (TNFa), interleukin 1a (IL1a), interleukin 17 (IL17f) and chemokine 2 (CCL2) in brain region homogenates after exposure to focused ultrasound.

While the acoustic pressure can lead to the ultrasound-sensitive release, there are different modes with the lowest pressure that could be utilized to deliver developed liposomes. We utilized focused ultrasound with Sonovue® microbubbles. We demonstrated that injection of fluorescently-labeled liposomes led to significant increase in fluorescence in comparison of perfused brain (Figure S4). The similar results were demonstrated by Zhuqing Song et al. who shown that TMZ-loaded liposomes could be successfully delivered across the BBB using microbubble-assisted FUS [39]. These results confirmed the potential of focused ultrasound in glioma therapy to work in two modes as an ultrasound-sensitive release and improved delivery by microbubble-assisted BBB opening.

© 2025 by the author(s). Distributed under a Creative Commons CC BY license.

Preprints.org (www.preprints.org) | NOT PEER-REVIEWED | Posted: 13 May 2025 doi:10.20944/preprints202505.0973.v1

3. Materials and Methods

3.1. Materials

Phosphatidylcholine (PC), Cholesterol, Dimethyldioctadecylammonium (Bromide Salt) (DDab) and 1,2 - distearoyl-sn-glycero-3-phosphoethanolamine-N-[amino(polyethyleneglycol)-2000] (ammonium salt) (DSPE-PEG 2000) were purchased from Avanti Lipids (USA). Methanol, chloroform, acetonitrile, formic acid, ammonium formate and ethanol were obtained from Chimmed (Russia). Dimethyl sulfoxide (DMSO), agarose, phosphate-buffer saline (PBS), penicillin/streptomycin and L-glutamine were purchased in Paneco (Russia). 1,1'-Dioctadecyl-3,3,3',3'-Tetramethylindodicarbocyanine and 4-Chlorobenzenesulfonate Salt (DID) were purchased from Lumiprobe (Russia). Temozolomide (TMZ) was purchased from TCI Shanghai (China). Oleic acid (OA) was obtained from Macklin Reagent Co., Ltd. (China). Sonovue was purchased from Bracco (Italy). Dulbecco's Modified Eagle Media (DMEM) was obtained from HiMedia (India). Fetal Bovine Serum (FBS) was obtained from Biowest (France). AlamarBlue® reagent was purchased from Thermo Fisher (USA). Hematoxylin and eosin (H&E) and formalin were obtained from Biovitrum (Russia). The primers, ExtractRNA, milli-Q H_2O, M-MLV Reverse Transcriptase kit and PCR Mix-HS SYBR Master Mix containing SYBR Green I dye were purchased from Evrogen (Russia). JetSpin™ centrifugal filters were obtained from Biofil (China). Acquity UPLC BEH Amide 2.1*150 mm column was purchased from Waters (USA). Dialysis bags (MWCO 3.5 kDa) were obtained from Spectra/Por (SpectrumLaboratories Inc., USA). Zoletil and xylazine were obtained from Virbac (France). Ultrasound (US) gel was purchased from Geltek (Russia). Isoflurane was obtained from Karizoo Laboratorios (Spain).

3.2. Cell Culture

GL261 cell lines were kindly provided by Dr. Aleksei Stepanenko from the Department of Fundamental and Applied Neurobiology of V. P. Serbsky Federal Medical Research Center of Psychiatry and Narcology. U87 cell line was obtained from ATCC. Cell cultures were grown in DMEM supplemented with 10% FBS, penicillin (500 units/ml), streptomycin (500 mkg/ml) and L-glutamine (0.4 M) in a 37^{0}C humidified incubator with 5% CO_2. Additionally, U-87 cells were cultured in collagen-coated plates. Each well in a 96-well plate was filled with 60 µl of Collagen Type I (32 µg/ml) and incubated for 30 minutes (37^{0}C, humidified 5% CO_2 atmosphere). Then, remaining collagen was removed and the wells were washed with PBS twice.

3.3. Setting up the Calibration Curves of TMZ and AIC

The standard concentration of TMZ (1 mg/ml) was diluted in PBS to stock concentrations from 1 to 100 µg/ml and measured for absorbance at 269 and 329 nm using fluorescent microplate reader (Varioskan Lux, Thermo Fisher, Waltham, MA, USA). The calibration curves were plotted by Prism 8 (GraphPad software, La Jolla, CA, USA).

3.4. Synthesis of Liposomal Formulations

3.4.1. Synthesis of Liposomes (Lip)

Two types of liposomes were synthesized by mixing cholesterol (1mg), PC, DSPE-PEG 2000 and DDab at different molar ratios (Table 1).

Table 1. Lipid composition of control liposomes (molar ratio).

Name	Cholesterol (%)	PC (%)	DSPE-PEG2000 (%)	DDab (%)
Lip	33.8	62.2	4.8	-
Lip-DDab	29.7	56	4.4	9.9

© 2025 by the author(s). Distributed under a Creative Commons CC BY license.

Preprints.org (www.preprints.org) | NOT PEER-REVIEWED | Posted: 13 May 2025 doi:10.20944/preprints202505.0973.v1

Combined lipids were dissolved in 5 ml of chloroform/ methanol (5:1) solution. The mixture was stirred for 1 hour on a magnetic stirrer of 750 rpm and then the solvent was removed by rotary evaporation. The formed lipid film was hydrated by adding 5 ml milli-Q H_2O and 5 mg of TMZ dissolved in 150 µl DMSO. Then the mixture was placed in an ultrasound water bath for 10 min at 45°C. The obtained liposomes were concentrated by ultrafiltration using JetSpin™ centrifugal filters (50 kDa) and stored for 4°C until further use.

3.4.2. Synthesis of OA-Based Liposomes (Lip-OA)

To evaluate the effect of OA on TMZ loading, different amounts of OA were used. Liposomes were prepared by mixing cholesterol (1mg), PC, DSPE-PEG 2000, OA and 8 mg TMZ (pre-dissolved in DMSO) at different molar ratios (Table 2).

Table 2. Lipid composition (molar ratio) of OA-based liposomes.

Name	Cholesterol (%)	PC (%)	DSPE-PEG (%)	Oleic acid (%)
Lip-OA 1:1	18.45	61.83	1.27	18.45
Lip-OA 1:10	6.93	23.24	0.48	69.35

Lipids were solved in chloroform/methanol solution (5:1) followed by evaporation under reduced pressure. The formed lipid films were hydrated by adding 5 ml milli-Q H_2O and for core shell liposomes 8 mg of TMZ was added. The films were then sonicated for 10 min. The obtained liposomes were concentrated by ultrafiltration using JetSpin™ centrifugal filters (30 kDa) and stored at 4°C until further use.

3.5. Physicochemical Characterization of Liposomes

The hydrodynamic diameter and polydispersity index (PDI) of liposomes were measured by dynamic light scattering (dls) using a Zetasizer Nano-S (Malvern Instruments, UK). Appropriate dilutions were made in PBS. The zeta potential was determined by assessing the mobility of the particles diluted in milli-Q H_2O in an applied electric field using a Zetasizer Nano-S (Malvern Instruments, UK). It was then calculated from the electrophoretic mobility based on the Helmholtz–Smoluchowski equation.

The concentration of TMZ and AIC was calculated according to their absorbance calibration curves by measuring the absorbance at 269 nm and 329 nm as described earlier.

Entrapment efficiency (EE, %) was calculated as the percent ratio of entrapped drug to the mass of drug loaded during synthesis via following equation:

$$EE = \frac{m_{loaded} - m_{encapsulated}}{m_{loaded}} 100$$

where m_{loaded} was mass of temozolomide added during synthesis and $m_{encapsulated}$ was mass of total drug (AIC and TMZ) determined with HPLC-MS.

3.6. Transmission Electron Microscopy (TEM)

Experiments were conducted using a JEOL JEM-1400 microscope (JEOL, Tokyo, Japan) operated at 120 kV acceleration voltage. Overview images were taken in conventional bright-field transmission mode. Samples were prepared by casting and evaporating a droplet of solution onto a carbon-coated copper grid (300 mesh). The samples were contrasted with Uranyless and lead citrate. The average diameter of liposomes was calculated from TEM images using ImageJ software.

3.7. High-Performance Liquid Chromatography - Mass Spectrometry (HPLC-MS)

To measure TMZ and AIC we have designed the original HPLC-MS method that utilizes hydrophilic interaction chromatography. Ultimate 3000 UHPLC system (Thermo Scientific) was coupled to the Acquity UPLC BEH Amide 2.1*150 mm column (Waters) and the Q-Exactive HF mass-

© 2025 by the author(s). Distributed under a Creative Commons CC BY license.

Preprints.org (www.preprints.org) | NOT PEER-REVIEWED | Posted: 13 May 2025 doi:10.20944/preprints202505.0973.v1

spectrometer working in positive ionization mode (Thermo Scientific). Chromatographic separation was accomplished in the following gradient of A and B solvents: 0-2 min: 1%B, 2-11 min: linear ramp from 1 to 50%B, 11-16 min: 50%B; where A was acetonitrile containing 5% water, 0.1% formic acid and 10 mM ammonium formate, and B was water containing the same concentrations of formic acid and ammonium formate as A. Dilution series of the TMZ and AIC standards have been prepared in 80% methanol in the 0.5 to 8.0 µg/ml concentration range with 2x steps and analyzed together with the samples to build calibration curves. Each sample and calibration curve point were 100x diluted with solvent A just before analysis and spiked with internal standard (theophylline) solution in 80% methanol to the final concentration of 120 nM. Mass-chromatograms have been collected in parallel reaction monitoring mode for the precursor ions with mass numbers 195.1 Th, 127.1 Th, 180.1 Th for TMZ, AIC and IS, respectively, isolated in a 1.6 Th mass window. Preliminary studies have shown that under selected fragmentation conditions the most intense fragments in the MS2 spectra of the above precursors have mass numbers of 138.041 Th, 110.035 Th, 124.051 Th, respectively. Therefore, they were selected as quantifiers for our analytes. The extracted ion chromatograms for these fragments were built and their chromatographic peak areas determined using FreeStyle 1.8.2 software (Thermo Scientific) for all samples and standard solutions. The quotient of the peak areas of the respective analyte and of the IS was the measure of the analyte quantity in the sample.

3.8. Stability Studies and Release Studies

3.8.1. Storage Stability

Colloidal stability of liposomes was assessed at 4°C (nanoparticle size and polydispersity) for a time period of 48 hours. At each time point, small aliquots were diluted and analyzed by DLS.

3.8.2. In Vitro Release Study

In vitro release study was performed using dialysis bags (MWCO 3.5 kDa). 1 ml of liposome suspension was loaded into bags and dialyzed against 20 ml of 0.01 M PBS buffer (pH 7.4) at 25^0C and 250 rpm. In 0.4, 0.5, 1, 2, 3, 4, 24 hours 300 µl samples of the buffer were taken to measure absorbance intensity at 269 nm and 329 nm as described earlier. TMZ and AIC concentrations were calculated using their absorbance calibration curves. Time-% of released drug curves were plotted using Prism 8 (GraphPad software, La Jolla, CA, USA).

3.9. In Vitro Cytotoxicity Assay

Cytotoxicity of TMZ and TMZ-loaded liposomes was studied on U-87 cell cultures using AlamarBlue® Assay according to the manufacturer's protocol. Cells (3000 cells per well) were seeded in 96-well plates and in 24 hours they were treated with either free TMZ or liposomes and incubated for 96 hours. After that the fluorescence was measured at 560/590 excitation/emission filter using a fluorescent microplate reader (Varioskan Lux, Thermo Fisher, Waltham, MA, USA). Concentration-response curves were plotted using Prism 8 (GraphPad software, La Jolla, CA, USA).

3.10. Selection of Parameters for Liposomes and LNP Destruction by FUS

Agarose based phantom was prepared to assess the parameters needed for the destruction of LNP by FUS. For that 2% agarose in distilled water was prepared in a 6-well plate and small cavities were made by 0.6 µl eppendorf for loading the water and thermocouple to measure the differences in temperature by FUS. The total exposure time and duty cycle were constant and comprised 60 sec and 5% respectively. The Pulse Repetition Frequency (PRF) was 1 and 5 Hz, the ultrasonic power varied from 6 to 15 V, that corresponds the pressure from 4.45 to 10.95 MPa.

3.11. Ultrasound Disruption of Liposomes and OA-Based Liposomes

The selected parameters were used to assess the destruction of LNP by FUS. For that the 2% agarose-based phantom with small pores for LNP was prepared. The thermocouple was used to

© 2025 by the author(s). Distributed under a Creative Commons CC BY license.

Preprints.org (www.preprints.org) | NOT PEER-REVIEWED | Posted: 13 May 2025 doi:10.20944/preprints202505.0973.v1

measure the temperature rise in the pores during the LNP destruction. The focused distance and duty cycle were 8 mm and 5% respectively. The PRF was 1 and 5 Hz at different pressures (5.11, 5.83, 7.30, 8.03, 9.13, 10, 10.59 and 11 MPa) with the exposure time 60 sec. The PDI of destructed LNP and graphs were demonstrated using Zetasizer Nano-S (Malvern Instruments, UK).

3.12. In Vivo Experiments

3.12.1. In Vivo Safety Experiment of Parameters of FUS

Several parameters of FUS were assessed in vivo for further use for delivery liposomes with TMZ by microbubbles without inducing any pathological changes. The Fvb mice were anesthetized (Zoletil (tiletamine + zolazepam) 20 mg/kg, xylazine 0.2 mg.kg), the heads were shaved and then a small amount of US gel was applied. After that the heads were induced by several parameters of FUS (Table 3). To provide a comprehensive understanding of the influence of FUS on the brain tissue the cytokine expression was analyzed by RT-PCR. The tissue integrity was assessed by MRI and the overall biological safety was evaluated through histological analysis.

Table 3. FUS parameters used for safety study in vivo on the brain tissue.

Group	Description	Duty Cycle	Pulse Repetition Frequency (PRF)	Pressure	Total Exposure Time
1	Control	-	-	-	-
2	Focused Ultrasound	5%	5 Hz	8.03 MPa	60 sec
3	Focused Ultrasound	5%	5 Hz	10 MPa	60 sec
4	Focused Ultrasound	5%	5 Hz	11 MPa	60 sec

3.12.2. Magnetic Resonance Imaging (MRI).

Magnetic Resonance Imaging (MRI) was conducted on mice three hours and three days after FUS exposure. The animals were anesthetized with 1.3% isoflurane during the procedure. The MR imaging utilized a T2 Turbo Spin Echo mode, with parameters set at TE/TR of 46/3720 ms, a slice thickness of 0.5 mm, and a resolution of 384/288 for the transversal plane. The imaging was carried out on a ClinScan 7T magnetic resonance tomography system (Bruker Biospin, USA). For the subsequent analysis of the data sets, Weasis DICOM viewer. Version 4.1.0 was employed (Roduit, N. https://github.com/nroduit/Weasis).

3.12.3. Histology

To collect the brain, tissue the mice were anesthetized (Zoletil (tiletamine + zolazepam) 20 mg/kg, xylazine 0.2 mg.kg) and then intravascular perfusion with 20 ml of PBS and then with 20 ml of 10% neutral-buffered formalin was performed. The collected brain samples were fixed in formalin for 24 hours. Following this fixation, the samples were rinsed with 70% ethanol before being embedded in paraffin using an embedding device. From the resulting paraffin blocks, two-micrometer-thick serial sections were sliced and subsequently stained with H&E dyes. These stained sections were then analysed under a light microscope Evos M5000 (Thermo Fisher Scientific, USA).

© 2025 by the author(s). Distributed under a Creative Commons CC BY license.

Preprints.org (www.preprints.org) | NOT PEER-REVIEWED | Posted: 13 May 2025 doi:10.20944/preprints202505.0973.v1

3.13. Real Time Polymerase Chain Reaction (RT-PCR).

Total RNA extraction was conducted using the ExtractRNA reagent, in accordance with the manufacturer's guidelines. A quantity of 1 μg of RNA was reverse-transcribed into cDNA using an MMLV kit with random primers. The temperature for this process was set at 60°C, and the duration was one hour. All quantitative polymerase chain reaction (qPCR) experiments were performed using the primers specified in Table S2. The qPCR reactions were prepared using the LightCycler 96 (Roche, Switzerland) and the qPCR Mix-HS SYBR Master Mix containing SYBR Green I dye. The following PCR cycle parameters were utilized: 95 °C for 180 seconds; 40 cycles of denaturation at 95 °C for 30 seconds, annealing at 62 °C for 30 seconds, and an extension step at 72 °C for 60 seconds.

The mRNA expression of the genes of interest were quantified using the 2-ΔΔCt method. Data were normalized to GAPDH mRNA level. The measurements were carried out in three technical replicates for each gene in three independent experiments.

4. Conclusions

Ultrasound-sensitive drug delivery systems offer a non-invasive and controlled method to trigger the release of therapeutic agents at the target site, minimizing systemic toxicity and enhancing local drug efficacy. In conclusion, we developed OA-modified liposomal formulations of TMZ with enhanced drug loading, sustained release, and increased sensitivity to FUS. OA incorporation significantly improved encapsulation efficiency and cytotoxicity in glioma cells, while enabling effective drug release at lower ultrasound pressures. In vivo studies confirmed that FUS parameters must be carefully controlled to avoid tissue damage. These results support OA-based liposomes as a promising platform for controlled, site-specific TMZ delivery in glioblastoma therapy.

Supplementary Materials: The following supporting information can be downloaded at: https://www.mdpi.com/article/doi/s1, Figure S1: TEM images of liposomes: A - 10000x; B - 20000x; Figure S2: Accumulation of cationic liposomes with TMZ labeled with fluorescent dye DiD in the brain (A) and biodistribution of liposomes in the heart, lungs, liver, spleen and kidney (B) after BBB opening by microbubbles using IVIS Spectrum CT. Lip-TMZ indicates the injection of liposomes with TMZ without induction of FUS, Lip-TMZ_FUS indicates the injection of liposomes with TMZ and FUS. Control group indicates a healthy mouse without injection and induction of FUS.; Figure S3: T2- weighted images of the brain of mice in control and after exposure to ultrasound (after 3 hours and 3 days).; Table S1: The selection of FUS parameters by the differences in the temperature.; Table S2: The primers sequences used in RT-PCR.

Author Contributions: T.O.A., V. S. S and N. S. Ch. wrote the main manuscript. T.O.A. performed design of the study and funding acquisition. V.D.D and I.M.Kh synthesized and characterized the nanoparticles. V.D.D performed the in vitro experiments. V.S.Sh and T.O.A. performed the destruction of the nanoparticles and in vivo experiments. N.S.Ch. obtained the images by transmission electron microscopy. D.A.K. measured TMZ and AIC concentrations by HPLC-MS. D.Yu.T. analyzed the mRNA expression by RT-PCR. V.V.B. – conceptualization and editing of the manuscript. All authors have read and agreed to the published version of the manuscript.

Funding: This work was supported by the grant Russian Science Foundation 22-75-10151.

Institutional Review Board Statement: All experiments were approved and conducted in accordance with institutional guidelines of Pirogov Russian National Research Medical University (Moscow, Russia, Approval 08/2023).

Data Availability Statement: The datasets used and analyzed during the study are available from the corresponding authors upon request.

Acknowledgments: We would like to thank Olga Patsap for histological staining. The MRI images were performed using the equipment of the Core Facility of Pirogov Russian National Research Medical University. We also would like to thank Sergey Titov for support in experiment with FUS.

© 2025 by the author(s). Distributed under a Creative Commons CC BY license.

Preprints.org (www.preprints.org) | NOT PEER-REVIEWED | Posted: 13 May 2025 doi:10.20944/preprints202505.0973.v1

Conflicts of Interest: The authors declare no conflicts of interest.

References

1. Miller, K.D.; Ostrom, Q.T.; Kruchko, C.; Patil, N.; Tihan, T.; Cioffi, G.; Fuchs, H.E.; Waite, K.A.; Jemal, A.; Siegel, R.L.; et al. Brain and Other Central Nervous System Tumor Statistics, 2021. *CA Cancer J Clin* **2021**, *71*, 381–406, doi:10.3322/caac.21693.
2. Price, M.; Ballard, C.; Benedetti, J.; Neff, C.; Cioffi, G.; Waite, K.A.; Kruchko, C.; Barnholtz-Sloan, J.S.; Ostrom, Q.T. CBTRUS Statistical Report: Primary Brain and Other Central Nervous System Tumors Diagnosed in the United States in 2017–2021. *Neuro Oncol* **2024**, *26*, vi1–vi85, doi:10.1093/neuonc/noae145.
3. Wei, Y.; Lv, J.; Zhu, S.; Wang, S.; Su, J.; Xu, C. Enzyme-Responsive Liposomes for Controlled Drug Release. *Drug Discov Today* **2024**, *29*, 104014, doi:10.1016/J.DRUDIS.2024.104014.
4. Lee, J.H.; Yeo, Y. Controlled Drug Release from Pharmaceutical Nanocarriers. *Chem Eng Sci* **2015**, *125*, 75–84, doi:10.1016/J.CES.2014.08.046.
5. Zheng, K.; Zhu, X.; Guo, S.; Zhang, X. Gamma-Ray-Responsive Drug Delivery Systems for Radiation Protection. *Chemical Engineering Journal* **2023**, *463*, 142522, doi:10.1016/J.CEJ.2023.142522.
6. Kumarasamy, R.V.; Natarajan, P.M.; Umapathy, V.R.; Roy, J.R.; Mironescu, M.; Palanisamy, C.P. Clinical Applications and Therapeutic Potentials of Advanced Nanoparticles: A Comprehensive Review on Completed Human Clinical Trials. *Frontiers in Nanotechnology* 2024, *6*.
7. Manini, I.; Caponnetto, F.; Dalla, E.; Ius, T.; Pepa, G.M. Della; Pegolo, E.; Bartolini, A.; Rocca, G. La; Menna, G.; Di Loreto, C.; et al. Heterogeneity Matters: Different Regions of Glioblastoma Are Characterized by Distinctive Tumor-Supporting Pathways. *Cancers (Basel)* **2020**, *12*, 1–24, doi:10.3390/cancers12102960.
8. Agarwala, S.S.; Kirkwood, J.M. Temozolomide, a Novel Alkylating Agent with Activity in the Central Nervous System, May Improve the Treatment of Advanced Metastatic Melanoma. *Oncologist* **2000**, *5*, 144–151, doi:10.1634/theoncologist.5-2-144.
9. Kumari, S.; Ahsan, S.M.; Kumar, J.M.; Kondapi, A.K.; Rao, N.M. Overcoming Blood Brain Barrier with a Dual Purpose Temozolomide Loaded Lactoferrin Nanoparticles for Combating Glioma (SERP-17-12433). *Sci Rep* **2017**, *7*, doi:10.1038/s41598-017-06888-4.
10. Fang, C.; Wang, K.; Stephen, Z.R.; Mu, Q.; Kievit, F.M.; Chiu, D.T.; Press, O.W.; Zhang, M. Temozolomide Nanoparticles for Targeted Glioblastoma Therapy. *ACS Appl Mater Interfaces* **2015**, *7*, 6674–6682, doi:10.1021/am5092165.
11. Liu, P.; Chen, G.; Zhang, J. A Review of Liposomes as a Drug Delivery System: Current Status of Approved Products, Regulatory Environments, and Future Perspectives. *Molecules* 2022, *27*.
12. Gabizon, A.A.; Gabizon-Peretz, S.; Modaresahmadi, S.; La-Beck, N.M. Thirty Years from FDA Approval of Pegylated Liposomal Doxorubicin (Doxil/Caelyx): An Updated Analysis and Future Perspective. *BMJ Oncology* 2025, *4*.
13. Amarandi, R.M.; Ibanescu, A.; Carasevici, E.; Marin, L.; Dragoi, B. Liposomal-Based Formulations: A Path from Basic Research to Temozolomide Delivery Inside Glioblastoma Tissue. *Pharmaceutics* 2022, *14*.
14. Waghule, T.; Laxmi Swetha, K.; Roy, A.; Narayan Saha, R.; Singhvi, G. Exploring Temozolomide Encapsulated PEGylated Liposomes and Lyotropic Liquid Crystals for Effective Treatment of Glioblastoma: In-Vitro, Cell Line, and Pharmacokinetic Studies. *European Journal of Pharmaceutics and Biopharmaceutics* **2023**, *186*, 18–29, doi:10.1016/J.EJPB.2023.03.004.
15. Iturrioz-Rodríguez, N.; Sampron, N.; Matheu, A. Current Advances in Temozolomide Encapsulation for the Enhancement of Glioblastoma Treatment. *Theranostics* **2023**, *13*, 2734–2756, doi:10.7150/thno.82005.

© 2025 by the author(s). Distributed under a Creative Commons CC BY license.

Preprints.org (www.preprints.org) | NOT PEER-REVIEWED | Posted: 13 May 2025 doi:10.20944/preprints202505.0973.v1

16. Maritim, S.; Boulas, P.; Lin, Y. Comprehensive Analysis of Liposome Formulation Parameters and Their Influence on Encapsulation, Stability and Drug Release in Glibenclamide Liposomes. *Int J Pharm* **2021**, *592*, 120051, doi:10.1016/J.IJPHARM.2020.120051.
17. Jang, E.J.; Choi, W.R.; Kim, S.Y.; Hong, S.S.; Rhee, I.; Lee, S.J.; Choi, S.W.; Choi, H.G.; Lim, S.J. 2-Hydroxyoleic Acid-Inserted Liposomes as a Multifunctional Carrier of Anticancer Drugs. *Drug Deliv* **2017**, *24*, 1587–1597, doi:10.1080/10717544.2017.1388452.
18. Gao, D.; Tang, S.; Tong, Q. Oleanolic Acid Liposomes with Polyethylene Glycol Modification: Promising Antitumor Drug Delivery. *Int J Nanomedicine* **2012**, *7*, 3517–3526, doi:10.2147/IJN.S31725.
19. Eh Suk, V.R.; Misran, M. Development and Characterization of DOPEPEG2000 Coated Oleic Acid Liposomes Encapsulating Anticancer Drugs. *J Surfactants Deterg* **2017**, *20*, 321–329, doi:10.1007/s11743-016-1914-8.
20. Huang, H.; Chen, Y.; Yin, N.; Li, G.; Ye, S.; Guo, L.; Feng, M. Unsaturated Fatty Acid Liposomes Selectively Regulate Glutathione Peroxidase 4 to Exacerbate Lipid Peroxidation as an Adaptable Liposome Platform for Anti-Tumor Therapy. *Mol Pharm* **2023**, *20*, 290–302, doi:10.1021/acs.molpharmaceut.2c00642.
21. Kurniawan, J.; Suga, K.; Kuhl, T.L. Interaction Forces and Membrane Charge Tunability: Oleic Acid Containing Membranes in Different PH Conditions. *Biochimica et Biophysica Acta (BBA) - Biomembranes* **2017**, *1859*, 211–217, doi:10.1016/J.BBAMEM.2016.11.001.
22. Dauba, A.; Delalande, A.; Kamimura, H.A.S.; Conti, A.; Larrat, B.; Tsapis, N.; Novell, A. Recent Advances on Ultrasound Contrast Agents for Blood-Brain Barrier Opening with Focused Ultrasound. *Pharmaceutics* 2020, *12*, 1–30.
23. Timbie, K.F.; Afzal, U.; Date, A.; Zhang, C.; Song, J.; Wilson Miller, G.; Suk, J.S.; Hanes, J.; Price, R.J. MR Image-Guided Delivery of Cisplatin-Loaded Brain-Penetrating Nanoparticles to Invasive Glioma with Focused Ultrasound. *Journal of Controlled Release* **2017**, *263*, 120–131, doi:10.1016/J.JCONREL.2017.03.017.
24. Li, Y.; North, R.Y.; Rhines, L.D.; Tatsui, C.E.; Rao, G.; Edwards, D.D.; Cassidy, R.M.; Harrison, D.S.; Johansson, C.A.; Zhang, H.; et al. Drg Voltage-Gated Sodium Channel 1.7 Is Upregulated in Paclitaxel-Induced Neuropathy in Rats and in Humans with Neuropathic Pain. *Journal of Neuroscience* **2018**, *38*, 1124–1136, doi:10.1523/JNEUROSCI.0899-17.2017.
25. Thapa Magar, K.; Boafo, G.F.; Li, X.; Chen, Z.; He, W. Liposome-Based Delivery of Biological Drugs. *Chinese Chemical Letters* **2022**, *33*, 587–596, doi:10.1016/J.CCLET.2021.08.020.
26. Hu, J.; Wang, J.; Wang, G.; Yao, Z.; Dang, X. Pharmacokinetics and Antitumor Efficacy of DSPE-PEG2000 Polymeric Liposomes Loaded with Quercetin and Temozolomide: Analysis of Their Effectiveness in Enhancing the Chemosensitization of Drug-Resistant Glioma Cells. *Int J Mol Med* **2016**, *37*, 690–702, doi:10.3892/ijmm.2016.2458.
27. Zhang, K.; Lv, S.; Li, X.; Feng, Y.; Li, X.; Liu, L.; Li, S.; Li, Y. Preparation, Characterization, and in Vivo Pharmacokinetics of Nanostructured Lipid Carriers Loaded with Oleanolic Acid and Gentiopicrin. *Int J Nanomedicine* **2013**, *8*, 3227–3239, doi:10.2147/IJN.S45031.
28. Gao, J.; Wang, Z.; Liu, H.; Wang, L.; Huang, G. Liposome Encapsulated of Temozolomide for the Treatment of Glioma Tumor: Preparation, Characterization and Evaluation. *Drug Discov Ther* **2015**, *9*, 205–212, doi:10.5582/ddt.2015.01016.
29. Almeleebia, T.M.; Akhter, M.H.; Khalilullah, H.; Rahman, M.A.; Ahmad, S.; Alam, N.; Ali, M.S.; Khan, G.; Alanazi, I.M.M.; Shahzad, N.; et al. Co-Delivery of Naringin and Ciprofloxacin by Oleic Acid Lipid Core Encapsulated in Carboxymethyl Chitosan/Alginate Nanoparticle Composite for Enhanced Antimicrobial Activity. *ACS Omega* **2024**, *9*, 6845–6860, doi:10.1021/acsomega.3c08200.

© 2025 by the author(s). Distributed under a Creative Commons CC BY license.

Preprints.org (www.preprints.org) | NOT PEER-REVIEWED | Posted: 13 May 2025 doi:10.20944/preprints202505.0973.v1

30. Latifah, L.; Hendradi, E.; Isadiartuti, D. Effect Ratio of Stearic Acid and Oleic Acid on Characteristics of Diclofenac Sodium Nanostructured Lipid Carrier. *Pharmacy Education* **2024**, *24*, 336–342, doi:10.46542/pe.2024.243.336342.
31. Kandagatla, H.P.; Kathawala, M.H.; Syed, A.; Verbić, T.Ž.; Avdeef, A.; Kuentz, M.; Serajuddin, A.T.M. Highly Increasing Solubility of Clofazimine, an Extremely Water-Insoluble Basic Drug, in Lipid-Based SEDDS Using Digestion Products of Long-Chain Lipids. *J Pharm Sci* **2025**, *114*, 103782, doi:10.1016/j.xphs.2025.103782.
32. Jatyan, R.; Sahel, D.K.; Singh, P.; Sakhuja, R.; Mittal, A.; Chitkara, D. Temozolomide-Fatty Acid Conjugates for Glioblastoma Multiforme: In Vitro and in Vivo Evaluation. *Journal of Controlled Release* **2023**, *359*, 161–174, doi:10.1016/J.JCONREL.2023.05.012.
33. Naik, A.; Pechtold, L.A.R.M.; Potts, R.O.; Guy, R.H. Mechanism of Oleic Acid-Induced Skin Penetration Enhancement in Vivo in Humans. *Journal of Controlled Release* **1995**, *37*, 299–306, doi:10.1016/0168-3659(95)00088-7.
34. Srisuk, P.; Thongnopnua, P.; Raktanonchai, U.; Kanokpanont, S. Physico-Chemical Characteristics of Methotrexate-Entrapped Oleic Acid-Containing Deformable Liposomes for in Vitro Transepidermal Delivery Targeting Psoriasis Treatment. *Int J Pharm* **2012**, *427*, 426–434, doi:10.1016/J.IJPHARM.2012.01.045.
35. Onuki, Y.; Hagiwara, C.; Sugibayashi, K.; Takayama, K. Specific Effect of Polyunsaturated Fatty Acids on the Cholesterol-Poor Membrane Domain in a Model Membrane. *Chem Pharm Bull (Tokyo)* **2008**, *56*, 1103–1109, doi:10.1248/cpb.56.1103.
36. Shashkovskaya, V.S.; Vetosheva, P.I.; Shokhina, A.G.; Aparin, I.O.; Prikazchikova, T.A.; Mikaelyan, A.S.; Kotelevtsev, Y. V.; Belousov, V. V.; Zatsepin, T.S.; Abakumova, T.O. Delivery of Lipid Nanoparticles with ROS Probes for Improved Visualization of Hepatocellular Carcinoma. *Biomedicines* **2023**, *11*, doi:10.3390/biomedicines11071783.
37. Schroeder, A.; Honen, R.; Turjeman, K.; Gabizon, A.; Kost, J.; Barenholz, Y. Ultrasound Triggered Release of Cisplatin from Liposomes in Murine Tumors. *Journal of Controlled Release* **2009**, *137*, 63–68, doi:10.1016/J.JCONREL.2009.03.007.
38. Schroeder, A.; Kost, J.; Barenholz, Y. Ultrasound, Liposomes, and Drug Delivery: Principles for Using Ultrasound to Control the Release of Drugs from Liposomes. *Chem Phys Lipids* **2009**, *162*, 1–16, doi:10.1016/J.CHEMPHYSLIP.2009.08.003.
39. Song, Z.; Huang, X.; Wang, J.; Cai, F.; Zhao, P.; Yan, F. Targeted Delivery of Liposomal Temozolomide Enhanced Anti-Glioblastoma Efficacy through Ultrasound-Mediated Blood–Brain Barrier Opening. *Pharmaceutics* **2021**, *13*, doi:10.3390/pharmaceutics13081270.

Disclaimer/Publisher's Note: The statements, opinions and data contained in all publications are solely those of the individual author(s) and contributor(s) and not of MDPI and/or the editor(s). MDPI and/or the editor(s) disclaim responsibility for any injury to people or property resulting from any ideas, methods, instructions or products referred to in the content.

© 2025 by the author(s). Distributed under a Creative Commons CC BY license.